Published in final edited form as:
J Med Genet. 2009 December ; 46(12): 803–810. doi:10.1136/jmg.2008.065961.

Clinical and cellular characterization of Hermansky-Pudlak syndrome type-6

Marjan Huizing[1], **Ben Pederson**[1], **Richard A Hess**[1], **Ashley Griffin**[1], **Amanda Helip-Wooley**[1], **Wendy Westbroek**[1], **Heidi Dorward**[1], **Kevin J O'Brien**[1,2], **Gretchen Golas**[1,2], **Ekaterini Tsilou**[3], **James G White**[4], and **William A Gahl**[1,2]

[1]Medical Genetics Branch, National Human Genome Research Institute, National Institutes of Health, Bethesda, USA

[2]Office of Rare Diseases, Intramural Program, Office of the Director, National Institutes of Health, Bethesda, USA

[3]Ophthalmic Genetics and Visual Function Branch, National Eye Institute, National Institutes of Health, Bethesda, USA

[4]Department of Laboratory Medicine, University of Minnesota, Minneapolis, USA

Abstract

Purpose—In the last decade, Hermansky-Pudlak syndrome (HPS) has arisen as an instructive disorder for cell biologists to study the biogenesis of lysosome-related organelles (LROs). Of the eight human HPS subtypes, only subtypes 1 through 5 are well described. Here, we carefully characterize the HPS-6 subtype, caused by defects in HPS6, a subunit of the biogenesis of lysosome-related organelles complex-2 (BLOC-2).

Methods—Mutation analysis for the *HPS6* gene was performed on DNA from our group of unclassified HPS patients. The clinical phenotype of patients with *HPS6* mutations was then carefully ascertained, and their cultured dermal melanocytes were employed for cellular immunofluorescence studies.

Results—Molecular studies showed a variety of mutations in the single-exon *HPS6* gene, including frame shift, missense, and nonsense mutations as well as a ~20-kb deletion spanning the entire *HPS6* gene. Cellular studies revealed that the melanogenic proteins tyrosinase and tyrosinase-related protein 1 failed to be efficiently delivered to the melanosomes of HPS-6 patients, explaining their hypopigmentation. Clinical studies indicated that HPS-6 patients exhibit oculocutaneous albinism and a bleeding diathesis. Importantly, granulomatous colitis and pulmonary fibrosis, debilitating features present in HPS subtypes 1 and 4, were not detected in our HPS-6 patients.

Conclusion—In sum, the HPS-6 subtype resembles other BLOC-2 defective subtypes (i.e., HPS-3 and HPS-5) in its molecular, cellular and clinical findings. These findings are not only important for providing a prognosis to newly diagnosed HPS-6 patients, but also for further elucidation of HPS function in the biogenesis of LROs.

Correspondence to: Marjan Huizing, PhD, Medical Genetics Branch, NHGRI, NIH, 10 Center Drive, MSC 1851, Building 10, Room 10C-103, Bethesda, Maryland 20892-1851, USA, TEL ++301-402-2797 FAX ++301-496-7184, mhuizing@mail.nih.gov.

Patients consent: Obtained from patient or patient's parent.

Competing interests: None declared.

Keywords

albinism; BLOC; lysosome-related organelle; melanosome; platelet

INTRODUCTION

Hermansky-Pudlak syndrome (HPS; MIM 203300) is an autosomal recessive disorder presenting with oculocutaneous albinism, a platelet storage pool deficiency and, in some cases, neutropenia, granulomatous colitis, or a fatal pulmonary fibrosis.[1] These clinical features result from defects in the synthesis, processing, or trafficking of lysosome-related organelles (LROs), which include melanosomes in melanocytes, delta granules in platelets, lamellar bodies in pulmonary type II cells, and secretory granules in T-cells.[2,3] To date, eight known human HPS genes have been identified; defects in these genes result in subtypes HPS-1 to HPS-8,[3,4] and each human subtype is associated with a murine model.[5]

The product of the HPS-2 gene, *AP3B1*, codes for the beta 3A subunit of adaptor complex-3 (AP-3), involved in vesicle formation and protein sorting.[6] The exact function of the other HPS gene products remains unknown. All known human HPS proteins interact with each other in biogenesis of lysosome-related organelles complexes (BLOCs); HPS1 and HPS4 form BLOC-3;[7,8] HPS3, HPS5 and HPS6 comprise BLOC-2;[9] and HPS7 and HPS8 are members of BLOC-1.[10–12] Human HPS subtypes involving defects in the same BLOC generally resemble each other clinically.[3,4] BLOC-3 deficient patients exhibit a relatively more severe phenotype of hypopigmentation, frequently develop granulomatous colitis, and are the only group who suffer a fatal pulmonary fibrosis.[3,4,13,14] Of the BLOC-2 deficient patients, only HPS-3 and HPS-5 have been studied in detail;[15,16] both have a milder phenotype of variable hypopigmentation and sporadic granulomatous colitis, but pulmonary fibrosis does not occur in HPS-3 or HPS-5 patients. So far, only two BLOC-1 patients have been reported, one HPS-7[10] and one HPS-8 family;[11] no detailed clinical features were provided apart from hypopigmentation and a bleeding diathesis.

An accurate diagnosis of the HPS subtype has important prognostic and treatment implications; the neutropenia in HPS-2 can be treated with G-CSF[17] and the pulmonary function in BLOC-3 patients can be addressed in studies of the small molecule pirfinidone.[18] Comprehensive genetic analysis of our NIH cohort of 232 HPS patients over the past decade resulted in detailed clinical and cellular descriptions of the HPS-1 [14,19–21], HPS-2[6,17], HPS-3[15,19], HPS-4[13], and HPS-5[16,22] subtypes.

A defect in *HPS6*, the human homologue of the murine *ruby-eye* gene, was initially identified in one patient.[23] Later we found *HPS6* to be defective in an Israeli Bedouin tribe.[24] Here we report extensive molecular analysis of *HPS6*, a single-exon gene located on chromosome 10q24.3. Using DNA from our group of unclassified HPS patients, we identified four HPS-6 patients and seven novel *HPS6* mutations. We ascertained the clinical phenotype of HPS-6 disease (MIM607522), and we employed HPS-6 patients' melanocytes for cellular studies.

PATIENTS AND METHODS

Patients and Cells

All patients were enrolled in a protocol approved by the National Human Genome Research Institute (NHGRI) institutional review board to evaluate the clinical and molecular aspects of HPS. Written informed consent was obtained from the patient or the patient's parent. The diagnosis of HPS was based on decreased visual acuity, nystagmus, hypopigmentation, and

the absence of platelet dense granules on whole-mount electron microscopy.[1] Primary cultures of epidermal melanocytes and fibroblasts were obtained from a forearm skin biopsy and cultured as previously described.[15,22]

Electron Microscopy of Platelet Dense Bodies

Platelet-rich plasma, prepared from fresh citrated blood, was placed on copper grids and treated as described.[1,15] The grids were air-dried and examined using a Philips model 301 electron microscope.

Molecular analysis

Genomic DNA and RNA were extracted from cultured fibroblasts or peripheral leukocytes as described.[15] Primers were designed to amplify the coding region, the 3'UTR and a part of the 5'UTR encoded by the single *HPS6* exon in nine overlapping fragments from genomic DNA (primer sequences available on request). Standard polymerase chain reaction (PCR) amplification procedures were employed. All PCR amplified products were directly sequenced using standard protocols. To verify allelic expression of the mutations in patient HPS115, a PCR fragment spanning both mutations was cloned into the TOPO TA Cloning Kit per the manufacturer's instructions (Invitrogen, Carlsbad, CA, USA). Individual clones were purified using the QIAprep Spin Miniprep Kit (Qiagen, Valencia, CA, USA) and subjected to sequence analysis.

Multiple Tissue Northern Blot Analysis

A human multiple tissue northern blot was obtained from Clontech (Palo Alto, CA, USA) and hybridized as described.[15] The *HPS6* probe was prepared by PCR-amplifying gDNA with primers 5′-GAAGCCCCACAGGGTGTTGAGTTG-3′ (nt 1250–1273) and 5′-GTGTCAGTGACACAGAGGAACTGT-3′ (nt 2478–2501) (GenBank NM_024747). In addition, the filter was probed with a β-actin probe (Clontech).

Copy number real-time quantitative PCR

TaqMan™ primers and probes (supplemental table S1) were ordered as pre-manufactured assays-on demand (*HPS6* assays Hs00544576_s1 and Hs00949672_s1) or custom designed for specific target sequences in the *HPS6* genomic region using the ABI Assay-by-Design service (Applied Biosystems, Foster City, CA, USA). Genomic DNA of patients HPS51 and HPS107 was PCR-amplified for the target sequences and for an endogenous control gene, *RNaseP*, on an ABI PRISM 7900 HT Sequence Detection System, following the manufacturer's recommendations (Applied Biosystems). Each PCR amplification was performed in triplicate and each experiment was repeated 3 times. The comparative Ct method was used to determine the target gene copy number in each sample.[25] The primer pair for amplification over the breakpoints of the deleted area in DNA of patient HPS107 were: P1, 5'-GGATGCTTGCCATGTTGCCC-3' and P2, 5'-GGATCCCGCCATGGTGTCCACC-3', yielding a fragment of 298-bp that was directly sequenced (fig 1F).

Immunocytochemistry

For steady state immunofluorescence (endogenous protein distribution), control and patient's melanocytes were grown overnight on glass chamber slides and fixed in 4% paraformaldehyde. The slides were blocked in PBS containing 0.1% saponin, 100 μM glycine, 0.1% BSA and 2% donkey serum then incubated with the following antibodies: mouse monoclonal MEL-5 recognizing TYRP1 (1:200 dilution; Signet Laboratories, Dedham, MA, USA), HMB45 detecting PMEL17 (1:200 dilution; Lab Vision, Fremont, CA, USA), and T311 detecting TYR (1:200; Santa Cruz Biotechnology, Santa Cruz, CA, USA).

The cells were subsequently washed and incubated with donkey anti-mouse antibodies conjugated to ALEXA-488 (Invitrogen), and nuclei were stained with TO-PRO-3 (Invitrogen). The cells were then rinsed and mounted in VectaShield (Vector Laboratories, Burlingame, CA, USA). For TYRP1 internalization studies, melanocytes were grown on glass slides and incubated for 30 min at 37°C in the presence of MEL-5 antibodies (1:200) diluted in DMEM containing 0.1% (wt/vol) BSA, and 25 mM HEPES buffer, pH 7.4. Subsequently, cells were washed in ice-cold PBS, fixed in 4% paraformaldehyde and incubated with secondary donkey anti-mouse ALEXA-488 antibodies (Invitrogen) and mounted as described above.

All slides were imaged with a Zeiss LSM510 META confocal laser-scanning microscope using 20X/.08 or 63X/1.4 Plan-Apochromat objectives (Carl Zeiss, Microimaging Inc., Germany). All images are collapsed stacks of confocal Z-sections. Fluorescence intensity plots (fig 4B) were created using Zeiss LSM software (Carl Zeiss, Microimaging Inc.). All images in figures 3 and 4 are representatives of three independent experiments.

RESULTS

Mutation analyses

Genomic DNA of our group of approximately 30 unclassified HPS patients was screened for mutations in *HPS6* by PCR amplification followed by direct sequencing. We identified *HPS6* mutations in four patients: HPS51, HPS107, HPS115, and HPS178 (fig 1, table 1).

Patient HPS51 displayed homozygosity for a novel two-base deletion, c.1865_1866delTG [p.L622RfsX12] resulting in a frameshift leading to a premature termination codon at amino acid position 633 with loss of nearly 20% of the HPS6 protein at the 3′ end (fig 1B). Patient HPS107 appeared homozygous for a novel nonsense mutation, c.913C>T [p.Q305X] (fig 1C). Patient HPS115 was compound heterozygous for a frameshift c.238dupG [p.D80GfsX96] and a missense mutation c.815C>T [p.T272I] (fig 1D). Amplification, subcloning and sequencing the *HPS6* region that included both mutations confirmed that the mutations were on separate alleles. The T272I missense mutation is not one of the two reported SNPs in *HPS6*; c.516G>A [p.G172G; rs3737243] and c.698T>G [p.L233R; rs36078476] (rs numbers refer to dbSNP database: http://www.ncbi.nlm.nih.gov/projects/SNP/), and sequencing of at least 90 alleles for *HPS6* mutations did not reveal this variant. Furthermore, the threonine at position 272 and its surrounding amino acids (VH**T**WAP) are conserved in other species (chimpanzee, horse, dog, pig, cow, rat, mouse, chicken), suggesting a functionally important amino acid. Patient HPS178 was compound heterozygous for two nonsense mutations, c.223C>T [p.Q75X] and c.1234C>T [p.Q412X] (fig 1E).

Both patients HPS51 and HPS107 appeared to be homozygous for a rare mutation, yet their families reported no consanguinity. Therefore, we investigated hemizygosity in these patients by copy number real-time PCR on genomic DNA, initially with two *HPS6* Taqman assays located in *HPS6* (assays *HPS6*ex1A and *HPS6*ex1B in fig 1F, supplemental table S1). Patient HPS51 had 2 allelic *HPS6* copies for each assay, similar to control DNA. However, patient HPS107 had only 1 allelic copy for each *HPS6* assay, and 2 allelic copies of the control gene (*RnaseP*), indicating hemizygosity in the *HPS6* region. To determine the dimension of this 10q24 deletion in patient HPS107, we performed copy number real-time PCR using a variety of Taqman primer-probe assays on either side of the deleted area (fig 1F, supplemental table S1). Two allelic copies were found for assays targeting the upstream gene *ORF67* (assay *ORF67*ex1) and the downstream gene *LBD1* (assay *LBD1*ex9). Subsequent assays targeting the upstream (5'UTR assays) and downstream (3'UTR assays) *HPS6* regions narrowed the deleted area to ~20kb located between *HPS6* 5UTRb and *HPS6*

3UTRc (fig 1F). We then tested combinations of primers on either side of the deletion to amplify across the deletion. Primers P1 and P2 yielded a 298-bp PCR fragment, and sequencing revealed the exact deletion breakpoints (fig 1F). The deletion covers 19,972-bp of genomic DNA, spanning the entire *HPS6* coding region, starting 2,659-bp upstream of the *HPS6* start codon (ATG) and ending 14,984-bp downstream of the *HPS6* termination codon (TGA). The breakpoints do not occur in a known genomic repeat area, but both breakpoint areas contain an identical 17-bp sequence: GCCATGTTGCCCAGGCT (fig 1F). This suggests that the deletion is a "simple deletion", meditated by a "symmetric element" mechanism involving short repetitive sequences present in the same direction on one allele.[26]

For patient HPS51 we sequenced of 6 single nucleotide polymorphic sites (SNPs) nearby on chromosome 10q24. All SNPs tested showed homozygosity, so uniparental disomy could not be excluded, but not further pursued since DNA from the patient's parents was not available.

HPS6 gene organization

HPS6 consists of 1 exon, located on chromosome 10q24.3. The open reading frame is predicted to code for a 775 amino acid, 83-kDa protein of unknown function. The protein is highly homologous to its mammalian orthologs, but lacks homology to any other proteins. No functional domains, leader sequence, or N-glycosylation sites are predicted. A multiple-tissue northern blot demonstrated that *HPS6* was expressed in all tissues tested, displaying a transcript size of approximately 2.6-kb, and no alternatively spliced transcripts were present (fig 2A). This ubiquitous expression is similar to that of other HPS genes[15,16] and was confirmed by a tissue microarray expression database (Stanford Microarray Database http://smd.stanford.edu/). Our attempts to create antibodies to the human HPS6 protein were unsuccessful, limiting further HPS6 protein analyses.

Cellular studies

Melanocytes are an ideal celltype to examine the biogenesis of lysosome-related organelles.[2,3,22,27] To evaluate the HPS-6 cellular phenotype, distributions of melanosomal proteins PMEL17, TYRP1, and TYR were assessed for patients HPS51 and HPS178 (fig 3). Patients' HPS51 and HPS178 melanocytes showed a dispersed cytoplasmic distribution of PMEL17, with accumulation in the dendritic tips, similar to the pattern in normal melanocytes (fig 3A). Normal melanocytes also showed a dispersed cellular pattern for TYRP1 and TYR, with accumulation in the dendritic tips (fig 3B,C left panels). However, TYRP1 and TYR distribution in the HPS-6 patients' melanocytes remained perinuclear, with decreased staining in the cell periphery and little or no accumulation in the dendritic tips (fig 3B,C, right panels). These aberrant patterns were similar to previously reported distribution of TYRP1 and TYR in BLOC-2 deficient human and mouse melanocytes,[22,28,29] following the hypothesis that PMEL17 is a resident protein of stage I and II melanosomes, where it serves as the structural foundation of fibrils upon which melanin can be deposited in later stage melanomomes.[2,30] Stage I and II melanosomes mature into stage III melanosomes by acquiring other melanogenic proteins and enzymes such as TYRP1 and TYR, which are crucial for melanin production, eventually resulting in a melanin-laden stage IV melanosome.[2,27,30] Endosomal transport of TYRP1 and TYR from the trans-Golgi complex into a sorting endosome is thought to be mediated by BLOC-3, while BLOC-2 is thought to play a role in further sorting and transport from the sorting endosome to stage II and III melanosomes.[2,27,29] Previous studies of BLOC-2 human (*HPS5* deficient[22]) and mouse (*cocoa, Hps3* deficient[28]) melanocytes showed enhanced flux of TYRP1 protein through the plasmamembrane and decreased steady-state TYRP1 levels due to lysosomal degradation of mistrafficked TYRP1. Our studies of HPS-6 melanocytes

yielded similar results; steady-state TYRP1 levels were decreased in HPS51 and HPS178 melanocytes (fig 3B), and TYRP1 internalization experiments revealed enhanced trafficking of TYRP1 through the plasma membrane leading to increased internalization of TYRP1 antibodies in HPS-6 melanocytes (fig 4).

Clinical Findings

Patient HPS51 is a 36-year old woman of Irish and German descent. At birth she had a 2-vessel umbilical cord, an imperforate anus with an anterior perineal fistula and abnormal eye movements. In early infancy, she had several urinary tract infections. At 5 months, an eye consultant found horizontal nystagmus and diagnosed partial albinism. The diagnosis of HPS was made at age 26 based upon eye findings and bleeding complications, and was confirmed by the finding of absent platelet dense bodies (fig 5D). The patient has a history of multiple abdominal surgeries for hernia, imperforate anus and gluteal flap repairs. Four units of packed red cells and several platelet transfusions were administered prior to these procedures. The patient bruises easily and has a bleeding time of 25.5 minutes. She has had four miscarriages, endometriosis, heavy menses, frequent upper respiratory and urinary tract infections, urinary and rectal incontinence with neurogenic bladder dysfunction, frequent migraines and hearing loss. On admission, the height was 161 cm, weight 92.5 kg, blood pressure 121/78. Hair color was light brown (fig 5A). Visual acuity was 20/100 in the right eye and 20/125 in the left. Iris transillumination was present (fig 5B), foveal reflex was absent and the fundus was pale (fig 5C). Whole mount electron microscopy of the platelets showed absent dense bodies (fig 5D). The forced vital capacity (FVC) was 94% of predicted, forced expiratory volume in 1 second (FEV_1) was 104% of predicted, and the total lung capacity for carbon monoxide (DL_{CO}) was 90% of predicted. The creatinine clearance was 129 $mL \cdot min^{-1} \cdot 1.73m^{-2}$ (normal 90–125). A chest radiogram was normal with no evidence of pulmonary fibrosis or interstitial lung disease. The serum cholesterol was 188 mg/dL (normal 100–200) and the triglycerides were 88 mg/dL (normal <150).

Patient HPS107 is a 22-year old man of Scottish, English, and German descent. Nystagmus was present at birth and the diagnosis of albinism was made at 3 months. As a toddler, the patient experienced prolonged bleeding and intermittent epistaxis; no other significant bleeding occurred. The diagnosis of HPS was made at age 16 based upon absence of platelet dense bodies (fig 5D). On admission, the height was 179 cm, weight 62 kg, and blood pressure 136/71. The hair was brown (fig 5A). Visual acuity was 20/80 in the right eye and and 20/63 in the left. There was transillumination of the irides (fig 5B) absence of foveal reflex and hypopigmentation of the fundi (fig 5C). The FVC was 104% of predicted, FEV_1 82% of predicted, and the DL_{CO} 77% of predicted. The creatinine clearance was 138 $mL \cdot min^{-1} \cdot 1.73m^{-2}$, the serum cholesterol was 143 mg/dL and triglycerides 306 mg/dL. The bleeding time was 9 minutes. Chest CT scan showed two small, nonspecific nodular densities, with no focal infiltrates.

Patient HPS115 is a 13-year old girl of German and Dutch descent. At 2 months of age she was noted to have mild horizontal nystagmus and was diagnosed with tyrosinase positive oculocutaneous albinism. Her hair, eyebrows and eyelashes were nearly white during the first year of life, but she developed some pigment later (fig 5A). She had strabismus surgery on both eyes at 14 months without major bleeding. After she began walking at 19 months, she was noted to bruise easily and have very slow nail growth. The patient has global developmental delay. At 14 months she was 6 months behind in both motor function and speech/language. She started using single words at 2–2.5 years of age and progressively acquired function over the next few years. At 4 years, the bleeding time was greater than 20 minutes, with normal von Willebrand factor, prothrombin time *(PT)* and partial thromboplastin time (PTT) tests. In vitro platelet aggregation responses to collagen, ADP

and arachidonic acid were all abnormal, prompting the diagnosis of platelet storage pool deficiency and HPS. Her platelets demonstrated absence of dense bodies (fig 5D), confirming the HPS diagnosis. She had no epistaxis or any other major bleeding events. At age 8, intravenous DDAVP and oral Amicar were used before dental work, which was performed without complications. On admission, the height was 137 cm (75%), weight 42.5 kg (97%), and blood pressure 107/52. Visual acuity was 20/200 bilaterally. The serum cholesterol was 141 mg/dL and the triglycerides 54 mg/dL.

Patient HPS178 is a 52-year old man from Italy. His two sisters have HPS, with symptomatic bleeding; one sister also has von Willebrand factor deficiency. The patient had rotatory nystagmus at birth and bruising in childhood. The diagnosis of HPS was made at age 44 bases upon the combination of gastrointestinal symptoms, nystagmus and oculocutaneous albinism. A pre-hernia repair evaluation at age 47 revealed a hemoglobin of 9 g/dL (normal 12.7–16.7). Iron and vitamin B_{12} deficiency were present. The patient had a history of esophageal dysmotility, hiatal hernia and other gastrointestinal complications including gastroesophageal reflux disease, dysphagia, and bloating. On admission, the blood pressure was 159/59. Visual acuity was 20/160 in the right eye and 20/125 in the left. The hair was light brown and the eyes dark brown (fig 5A). His irides showed transillumination (fig 5B). The FVC was 105% of predicted, FEV_1 112% of predicted, and the DL_{CO} 105% of predicted. The creatinine clearance was 130 $mL \cdot min^{-1} \cdot 1.73m^{-2}$, the serum cholesterol 96 mg/dL and triglycerides 79 mg/dL. Chronic inflammation due to recurrent gastrointestinal complications and an elevated C-reactive protein suggested that his anemia was chronic; it was not considered due to vitamin or iron deficiencies. Chest, abdomen and pelvis CT scans showed a calcified granuloma and a few nonspecific, subcentimeter irregular focal densities in the lung. No evidence of interstitial lung disease was detected.

DISCUSSION

Careful evaluation of our group of HPS-6 patients revealed that they appear to have clinical features similar to those of other BLOC-2 deficient patients, i.e., patients with HPS-3[15] and HPS-5,[16] including variable hypopigmentation and bleeding diathesis. Importantly, HPS-6 patients showed no signs of granulomatous colitis or pulmonary fibrosis, which are common features in BLOC-3 deficient patients with HPS-1 and HPS-4.[1,13,14,20,21] Specifically, two patients (HPS107 and HPS115) were of an age at which lung disease typically develops in BLOC-3 deficient patients. It is therefore imperative that adults with HPS-6 continue to be followed for the development of restrictive lung disease in order to determine whether pulmonary involvement occurs in this subtype and to anticipate therapy.[18]

Molecular findings indicated a variety of *HPS6* mutations scattered throughout the gene (fig 1A, table 1). All mutations were nonsense or frame-shift, likely resulting in aberrant protein translation. However, one missense mutation, p.T272I, was located in a conserved HPS6 region, possibly indicating significance for HPS6 function. Molecular studies on patient HPS107 demonstrated the importance of considering hemizygosity when a DNA alteration appears to be homozygous. Confirmation of hemizygosity can eliminate concerns about nonpaternity and can help explain other clinical features if the deleted area includes other genes.

Cellular studies performed on HPS-6 melanocytes indicated similar aberrant distribution and trafficking patterns of the melanogenic proteins TYRP1 and TYR (fig 3, 4), as described for other BLOC-2 deficient (HPS3 and HPS5) melanocytes. These findings confirmed that the BLOC-2 subunits HPS3, HPS5 and HPS6 act in the same pathway of LRO biogenesis. Thus, if melanocytes are available, immunofluorescent microscopy may help in diagnosing BLOC-2 deficiency, and focus genetic analyses on the *HPS3, HPS5* and *HPS6* genes. These

cellular studies again denote the value of cultured melanocytes for research of LROs[2,3,27] and we encourage that, when possible, a melanocyte culture is grown from skin biopsies of patients with LRO disorders. These cells will be invaluable sources for future investigations into the biogenesis of LROs.

Supplementary Material

Refer to Web version on PubMed Central for supplementary material.

Acknowledgments

Isa Bernardini, Roxanne Fischer, and David Claassen provided excellent technical assistance.

Funding: This work was supported by the Intramural Research programs of the National Human Genome Research Institute, National Institutes of Health, Bethesda, MD, USA.

REFERENCES

1. Gahl WA, Brantly M, Kaiser-Kupfer MI, Iwata F, Hazelwood S, Shotelersuk V, Duffy LF, Kuehl EM, Troendle J, Bernardini I. Genetic defects and clinical characteristics of patients with a form of oculocutaneous albinism (Hermansky-Pudlak syndrome). N Engl J Med. 1998; 338:1258–1264. [PubMed: 9562579]
2. Raposo G, Marks MS, Cutler DF. Lysosome-related organelles: driving post-Golgi compartments into specialisation. Curr Opin Cell Biol. 2007; 19:394–401. [PubMed: 17628466]
3. Huizing M, Helip-Wooley A, Westbroek W, Gunay-Aygun M, Gahl WA. Disorders of Lysosome-Related Organelle Biogenesis: Clinical and Molecular Genetics. Annu Rev Genomics Hum Genet. 2008; 9:359–386. [PubMed: 18544035]
4. Wei ML. Hermansky-Pudlak syndrome: a disease of protein trafficking and organelle function. Pigment Cell Res. 2006; 19:19–42. [PubMed: 16420244]
5. Li W, Rusiniak ME, Chintala S, Gautam R, Novak EK, Swank RT. Murine Hermansky-Pudlak syndrome genes: regulators of lysosome-related organelles. Bioessays. 2004; 26:616–628. [PubMed: 15170859]
6. Dell'Angelica EC, Shotelersuk V, Aguilar RC, Gahl WA, Bonifacino JS. Altered trafficking of lysosomal proteins in Hermansky-Pudlak syndrome due to mutations in the beta 3A subunit of the AP-3 adaptor. Mol Cell. 1999; 3:11–21. [PubMed: 10024875]
7. Martina JA, Moriyama K, Bonifacino JS. BLOC-3, a protein complex containing the Hermansky-Pudlak syndrome gene products HPS1 and HPS4. J Biol Chem. 2003; 278:29376–29384. [PubMed: 12756248]
8. Nazarian R, Falcon-Perez JM, Dell'Angelica EC. Biogenesis of lysosome-related organelles complex 3 (BLOC-3): a complex containing the Hermansky-Pudlak syndrome (HPS) proteins HPS1 and HPS4. Proc Natl Acad Sci U S A. 2003; 100:8770–8775. [PubMed: 12847290]
9. Di Pietro SM, Falcon-Perez JM, Dell'Angelica EC. Characterization of BLOC-2, a complex containing the Hermansky-Pudlak syndrome proteins HPS3, HPS5 and HPS6. Traffic. 2004; 5:276–283. [PubMed: 15030569]
10. Li W, Zhang Q, Oiso N, Novak EK, Gautam R, O'Brien EP, Tinsley CL, Blake DJ, Spritz RA, Copeland NG, Jenkins NA, Amato D, Roe BA, Starcevic M, Dell'Angelica EC, Elliott RW, Mishra V, Kingsmore SF, Paylor RE, Swank RT. Hermansky-Pudlak syndrome type 7 (HPS-7) results from mutant dysbindin, a member of the biogenesis of lysosome-related organelles complex 1 (BLOC-1). Nat Genet. 2003; 35:84–89. [PubMed: 12923531]
11. Morgan NV, Pasha S, Johnson CA, Ainsworth JR, Eady RA, Dawood B, McKeown C, Trembath RC, Wilde J, Watson SP, Maher ER. A germline mutation in BLOC1S3/reduced pigmentation causes a novel variant of Hermansky-Pudlak syndrome (HPS8). Am J Hum Genet. 2006; 78:160–166. [PubMed: 16385460]

12. Starcevic M, Dell'Angelica EC. Identification of snapin and three novel proteins (BLOS1, BLOS2, and BLOS3/reduced pigmentation) as subunits of biogenesis of lysosome-related organelles complex-1 (BLOC-1). J Biol Chem. 2004; 279:28393–28401. [PubMed: 15102850]

13. Anderson PD, Huizing M, Claassen DA, White J, Gahl WA. Hermansky-Pudlak syndrome type 4 (HPS-4): clinical and molecular characteristics. Hum Genet. 2003; 113:10–17. [PubMed: 12664304]

14. Hermos CR, Huizing M, Kaiser-Kupfer MI, Gahl WA. Hermansky-Pudlak syndrome type 1: gene organization, novel mutations, and clinical-molecular review of non-Puerto Rican cases. Hum Mutat. 2002; 20:482. [PubMed: 12442288]

15. Huizing M, Anikster Y, Fitzpatrick DL, Jeong AB, D'Souza M, Rausche M, Toro JR, Kaiser-Kupfer MI, White JG, Gahl WA. Hermansky-Pudlak syndrome type 3 in Ashkenazi Jews and other non-Puerto Rican patients with hypopigmentation and platelet storage-pool deficiency. Am J Hum Genet. 2001; 69:1022–1032. [PubMed: 11590544]

16. Huizing M, Hess R, Dorward H, Claassen DA, Helip-Wooley A, Kleta R, Kaiser-Kupfer MI, White JG, Gahl WA. Cellular, molecular and clinical characterization of patients with Hermansky-Pudlak syndrome type 5. Traffic. 2004; 5:711–722. [PubMed: 15296495]

17. Fontana S, Parolini S, Vermi W, Booth S, Gallo F, Donini M, Benassi M, Gentili F, Ferrari D, Notarangelo LD, Cavadini P, Marcenaro E, Dusi S, Cassatella M, Facchetti F, Griffiths GM, Moretta A, Notarangelo LD, Badolato R. Innate immunity defects in Hermansky-Pudlak type 2 syndrome. Blood. 2006; 107:4857–4864. [PubMed: 16507770]

18. Gahl WA, Brantly M, Troendle J, Avila NA, Padua A, Montalvo C, Cardona H, Calis KA, Gochuico B. Effect of pirfenidone on the pulmonary fibrosis of Hermansky-Pudlak syndrome. Mol Genet Metab. 2002; 76:234–242. [PubMed: 12126938]

19. Tsilou ET, Rubin BI, Reed GF, McCain L, Huizing M, White J, Kaiser-Kupfer MI, Gahl W. Milder ocular findings in Hermansky-Pudlak syndrome type 3 compared with Hermansky-Pudlak syndrome type 1. Ophthalmology. 2004; 111:1599–1603. [PubMed: 15288994]

20. Hussain N, Quezado M, Huizing M, Geho D, White JG, Gahl W, Mannon P. Intestinal disease in Hermansky-Pudlak syndrome: occurrence of colitis and relation to genotype. Clin Gastroenterol Hepatol. 2006; 4:73–80. [PubMed: 16431308]

21. Avila NA, Brantly M, Premkumar A, Huizing M, Dwyer A, Gahl WA. Hermansky-Pudlak syndrome: radiography and CT of the chest compared with pulmonary function tests and genetic studies. AJR Am J Roentgenol. 2002; 179:887–892. [PubMed: 12239031]

22. Helip-Wooley A, Westbroek W, Dorward HM, Koshoffer A, Huizing M, Boissy RE, Gahl WA. Improper trafficking of melanocyte-specific proteins in Hermansky-Pudlak syndrome type-5. J Invest Dermatol. 2007; 127:1471–1478. [PubMed: 17301833]

23. Zhang Q, Zhao B, Li W, Oiso N, Novak EK, Rusiniak ME, Gautam R, Chintala S, O'Brien EP, Zhang Y, Roe BA, Elliott RW, Eicher EM, Liang P, Kratz C, Legius E, Spritz RA, O'Sullivan TN, Copeland NG, Jenkins NA, Swank RT. Ru2 and Ru encode mouse orthologs of the genes mutated in human Hermansky-Pudlak syndrome types 5 and 6. Nat Genet. 2003; 33:145–153. [PubMed: 12548288]

24. Schreyer-Shafir N, Huizing M, Anikster Y, Nusinker Z, Bejarano-Achache I, Maftzir G, Resnik L, Helip-Wooley A, Westbroek W, Gradstein L, Rosenmann A, Blumenfeld A. A new genetic isolate with a unique phenotype of syndromic oculocutaneous albinism: clinical, molecular, and cellular characteristics. Hum Mutat. 2006; 27:1158. [PubMed: 17041891]

25. Livak KJ, Schmittgen TD. Analysis of relative gene expression data using real-time quantitative PCR and the 2(-Delta Delta C(T)) Method. Methods. 2001; 25:402–408. [PubMed: 11846609]

26. Chuzhanova N, Abeysinghe SS, Krawczak M, Cooper DN. Translocation and gross deletion breakpoints in human inherited disease and cancer II: Potential involvement of repetitive sequence elements in secondary structure formation between DNA ends. Hum Mutat. 2003; 22:245–251. [PubMed: 12938089]

27. Raposo G, Tenza D, Murphy DM, Berson JF, Marks MS. Distinct protein sorting and localization to premelanosomes, melanosomes, and lysosomes in pigmented melanocytic cells. J Cell Biol. 2001; 152:809–824. [PubMed: 11266471]

28. Di Pietro SM, Falcon-Perez JM, Tenza D, Setty SR, Marks MS, Raposo G, Dell'Angelica EC. BLOC-1 interacts with BLOC-2 and the AP-3 complex to facilitate protein trafficking on endosomes. Mol Biol Cell. 2006; 17:4027–4038. [PubMed: 16837549]

29. Setty SR, Tenza D, Truschel ST, Chou E, Sviderskaya EV, Theos AC, Lamoreux ML, Di Pietro SM, Starcevic M, Bennett DC, Dell'Angelica EC, Raposo G, Marks MS. BLOC-1 is required for cargo-specific sorting from vacuolar early endosomes toward lysosome-related organelles. Mol Biol Cell. 2007; 18:768–780. [PubMed: 17182842]

30. Berson JF, Harper DC, Tenza D, Raposo G, Marks MS. Pmel17 initiates premelanosome morphogenesis within multivesicular bodies. Mol Biol Cell. 2001; 12:3451–3464. [PubMed: 11694580]

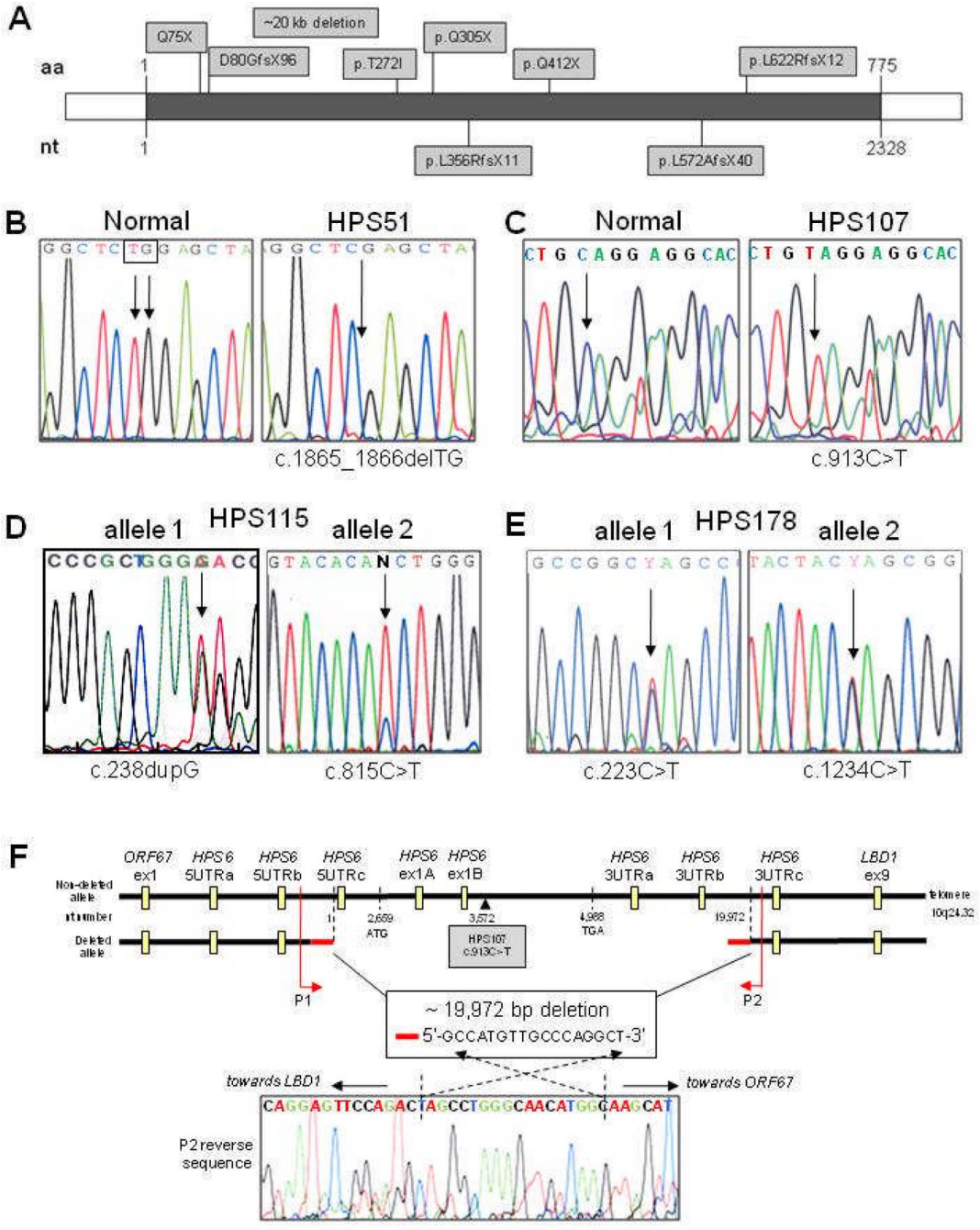

Figure 1.

Molecular analysis of HPS-6 patients. (A) All identified mutations in *HPS6* to date, indicated by amino acid change. Mutations denoted above the *HPS6* gene (grey line) are novel mutations described in this paper. Mutations below the *HPS6* gene were previously reported. *aa*=amino acid; *nt*=nucleotide. (B) Patient HPS51 was homozygous for c. 1865_1866delTG [p.L622RfsX12]. (C) Patient HPS107 was hemizygous for c.913C>T [p.Q305X]. (D) Patient HPS115 was compound heterozygous for a frameshift c.238dupG [p.D80GfsX96] (left panel) and a missense mutation c.815C>T [p.T272I] (right panel). (E) Patient HPS178 was compound heterozygous for two nonsense mutations: c.223C>T [p.Q75X] (left panel) and c.1234C>T [p.Q412X] (right panel). (F) Schematic of the 19,972-

bp deletion in patient HPS107 (not to scale). Deletion breakpoints, size, overlapping sequence and positions of the Taqman copy number assays are indicated. Primers P1 and P2 were used to sequence across the deletion; the *reverse* sequence acquired with the P2 primer, including the overlapping 17-bp sequence is shown.

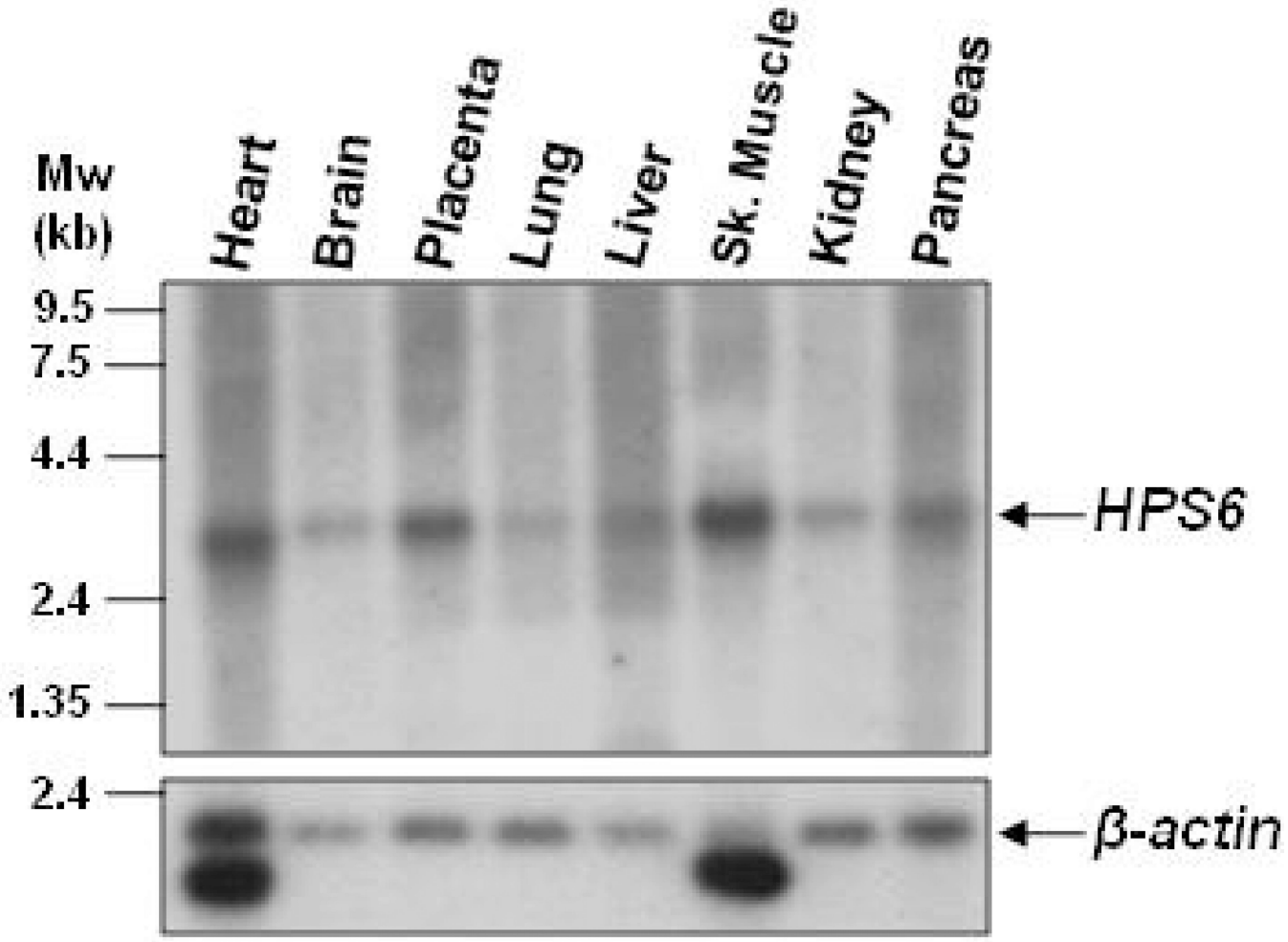

Figure 2.
HPS6 mRNA expression. A multiple tissue Northern blot hybridized with a [^{32}P]dCTP-labeled *HPS6* probe demonstrating a ~2.6-kb *HPS6* mRNA transcripts in all tissues tested (*upper panel*). The blot was subsequently hybridized with a [^{32}P]dCTP-labeled β-actin probe to control for RNA loading (*lower panel*).

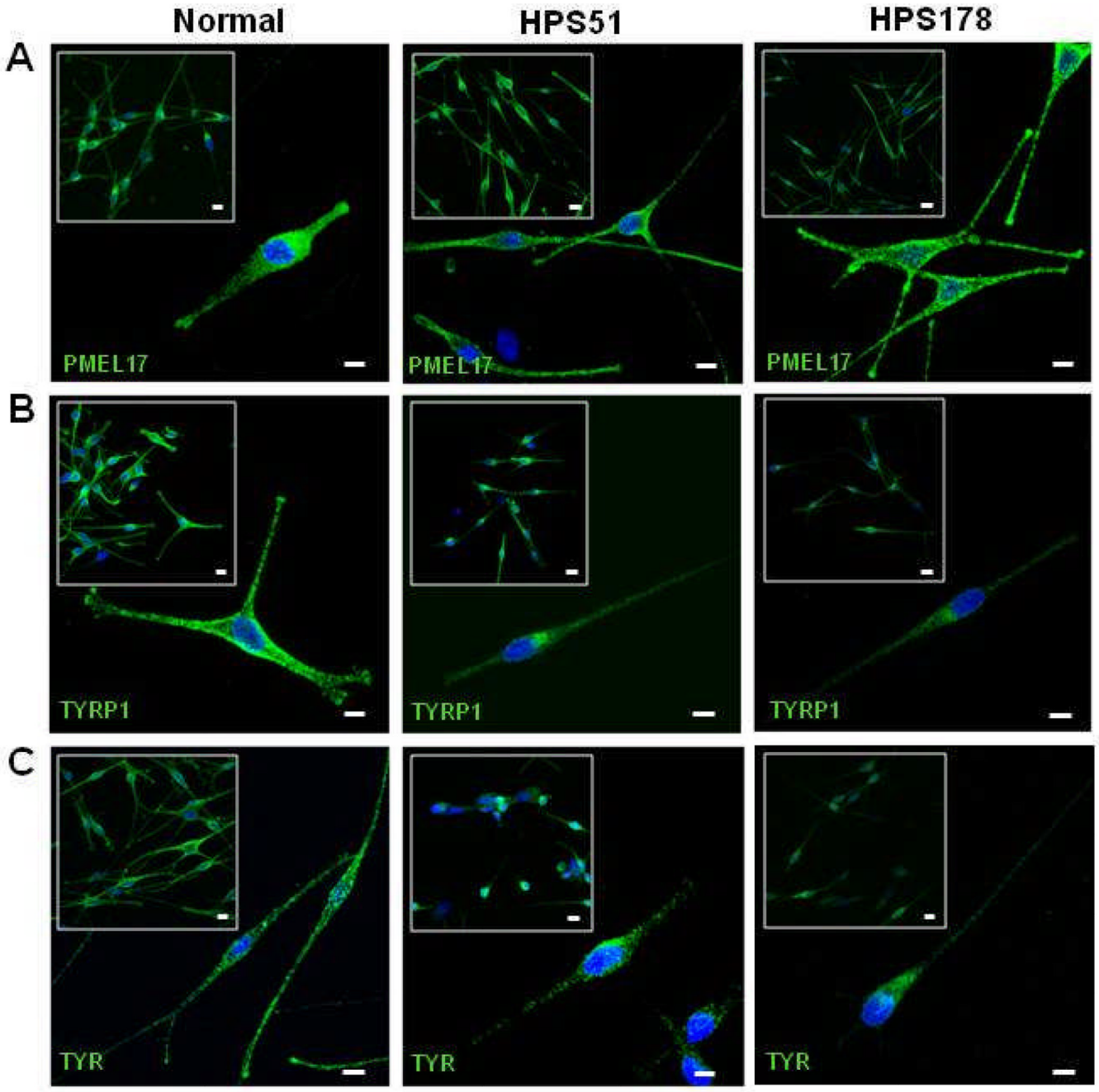

Figure 3.

Steady-state distribution of melanogenic markers PMEL17, TYRP1, and TYR in normal and HPS-6 patients' melanocytes (HPS51 and HPS178). (A) PMEL17 (HMB45, green) is normally distributed throughout the perinuclear region and accumulates in the tips in HPS-6 melanocytes. (B) TYRP1 (MEL5, green) is concentrated in the perinuclear region and fails to extend into the dendrites and does not accumulate in the tips of HPS-6 melanocytes. Intensity of TYRP1 signals in HPS-6 cells is decreased due to lysosomal degradation of mistrafficked TYRP1.[22,28] (C) TYR (T311, green) is concentrated in the perinuclear region and does not extend into the dendrites and tips of HPS-6 melanocytes.

All cell nuclei are stained with TO-PRO-3 (blue). Images represent collapsed stacks of confocal z-sections. Sizebars = 10 μm; Sizebars in insets = 20 μm.

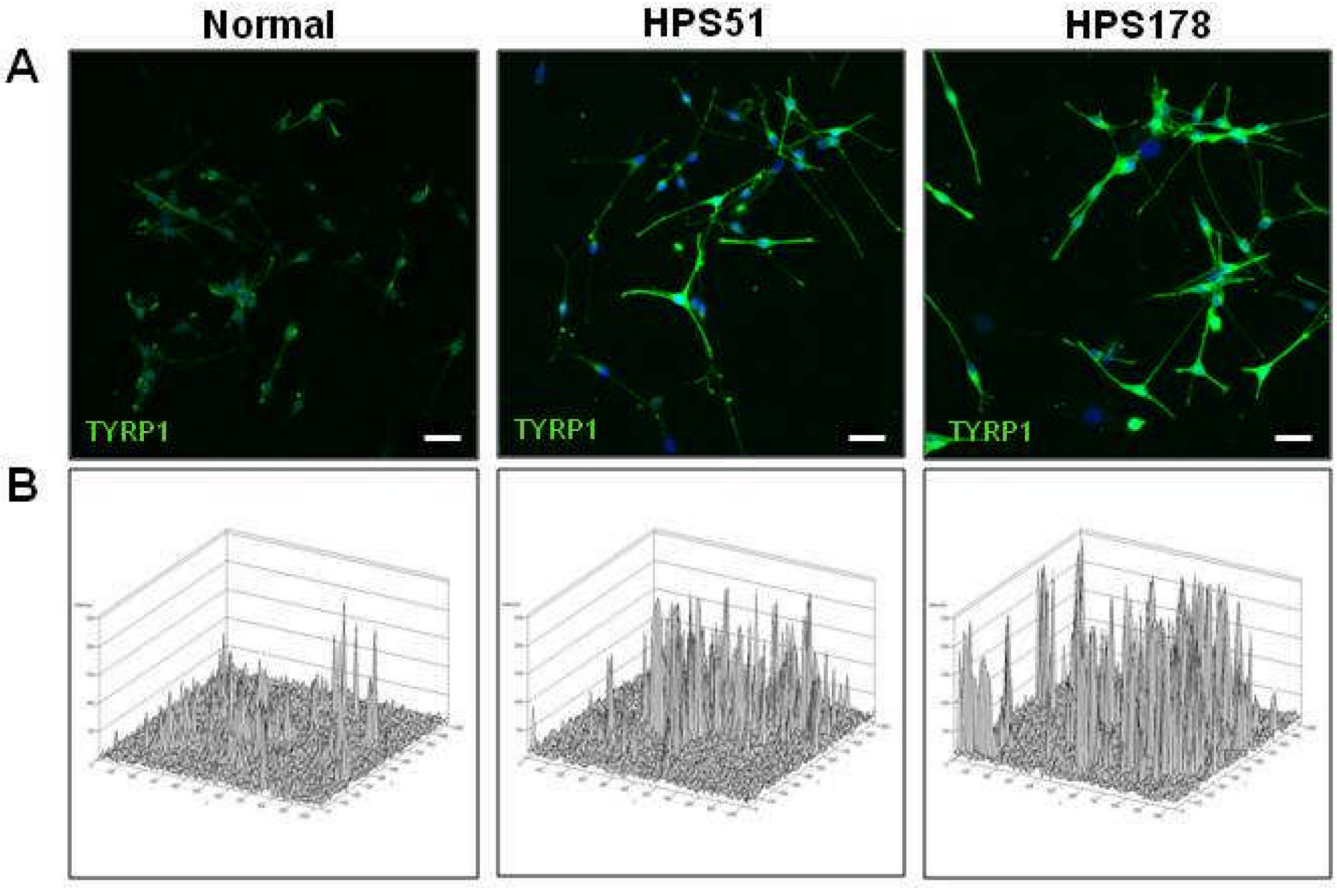

Figure 4.

TYRP1 antibody internalization studies on HPS-6 melanocytes. (A) Trafficking of TRYP1 (green) via the cell membrane is markedly increased in HPS-6 melanocytes (HPS51 and HPS178) compared to normal melanocytes (left panel), as illustrated by TYRP1 antibody incubation for 30 min in unpermeabilized cells. Cell nuclei are stained with TO-PRO-3 (blue). Images represent collapsed stacks of confocal z-sections. Sizebars = 20 μm. (B) Fluorescence intensity plots of the images in (A) (green channel only).

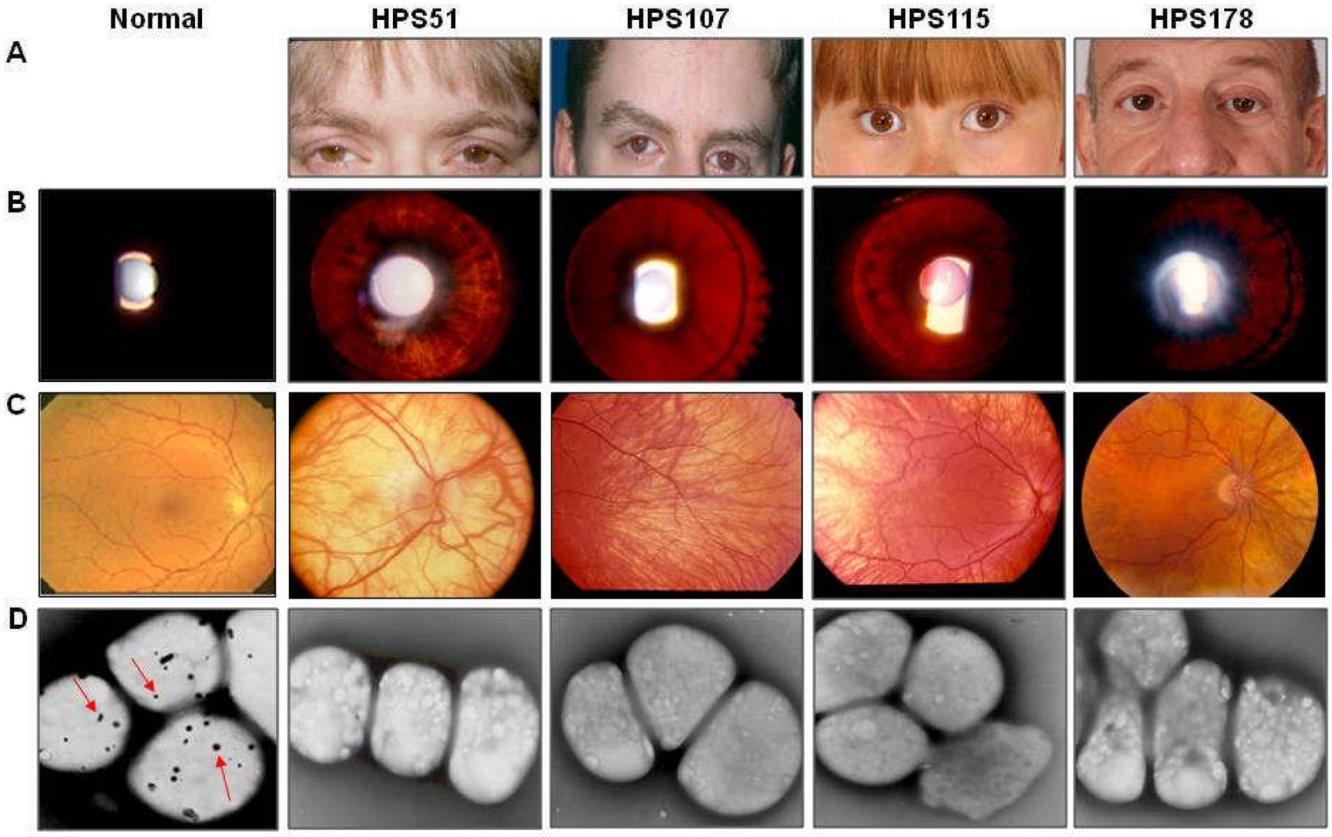

Figure 5.

Clinical features of HPS-6 patients. (A) Skin and hair show variable extents of hypopigmentation. (B) Iris transillumination is caused by light that is transmitted back through the iris when light is shone through the pupil. A normal iris remains dark (*left panel*). All four HPS-6 patients show light transmitted back as a result of reduced iris pigmentation. (C) Contrasting with the normal, uniform pigmentation (*left panel*), each HPS-6 patient has variable degrees of hypopigmentation of the retina. (D) Whole mount electron micrographs of platelets (× 10,000–13,000). Normal platelets contain several delta granules per platelet (*left panel*, arrows), while HPS-6 platelets lack delta granules.

Table 1

HPS6 mutations and patients' ancestries

Allele	Amino acid change	Ethnic background	Reference
c.223C>T	p.Q75X	Italian	This report HPS178
c.238dupG	p.D80GfsX96	German/Dutch	This report HPS115
c.815C>T	p.T272I	German/Dutch	This report HPS115
c.913C>T	p.Q305X	Scottish/English/German	This report HPS107
c.1066-1067insG	p.L356RfsX11	Israeli Bedioun	[24]
c.1234C>T	p.Q412X	Italian	This report HPS178
c.1718_1722delTCTG	p.L572AfsX40	Belgium	[23]
c.1865_1866delTG	p.L622RfsX12	Irish/German	This report HPS51
del 19,972-bp	-	Scottish/English/German	This report HPS107